Large-Signal Modeling of Hysteretic Current-Programmed Converters

Yan-Fei Liu, *Member, IEEE,* and Paresh C. Sen, *Fellow, IEEE*

***Abstract*—Large-signal dynamic models for hysteretic current-programmed buck, boost, and buck-boost converters are proposed. The model is expressed by a single differential equation. The small-signal transfer functions of these three converters are also derived, based on the large-signal model. The analysis shows that under the hysteretic current-programmed control, the output voltage of the buck converter is independent of the supply voltage, and there is a right-half plane (RHP) zero in the control-to-output transfer function of boost and buck-boost converters. An experimental prototype is breadboarded to verify the analysis.**

I. Introduction

CURRENT-PROGRAMMED control offers significant improvement over conventional direct duty ratio control and is becoming more widely used in industrial applications. In current-programmed control, the control signal to the switching converter tries to control the inductor current directly. The duty ratio of the switch is controlled only indirectly. Among the various types of current-programmed control, the hysteretic current-programmed control [1], [2] offers the tightest control of the inductor current and the fastest possible response of the inductor current.

In the hysteretic current-programmed control [1], as shown in Fig. 1, the switch is turned off when the inductor current rises to its peak value determined by $i_{cp} = i_c + \Delta I/2$, where i_c is the control signal and ΔI is the desired inductor current ripple. When the inductor current falls to its minimum, $i_{cv} = i_c - \Delta I/2$, the switch is turned on. Another description of the hysteretic current-programmed control is that when the inductor current rises to the control signal, i_c, the switch is turned off, and when the inductor current falls to $i_c - \Delta I$, the switch is turned on again. These two descriptions are actually the same. The authors of the paper prefer the first description because it would lead to simpler expressions in the dynamic analysis.

In the hysteretic current-programmed control, the inductor current i_L is tightly controlled by the control signal i_c. Another advantage is that there is no subharmonic oscillation in the hysteretic current-programmed control.

Some efforts have been made to analyze the small-signal dynamic characteristics of the hysteretic current-programmed control [1], [2], [8]. Small-signal transfer functions of the hysteretic current programmed converters, which can be used to design the feedback compensation loop, have been derived.

Manuscript received November 29, 1993; revised January 17, 1996.

Y.-F. Liu is with Nortel Technologies, , Ottawa, Ontario, K1Y 4H7 Canada.
P. C. Sen is with Queen's University, Department of Electrical Engineering, Power Electronics and Drives Lab, Kingston, Ontario K7L 3N6, Canada.

Publisher Item Identifier S 0885-8993(96)03554-5.

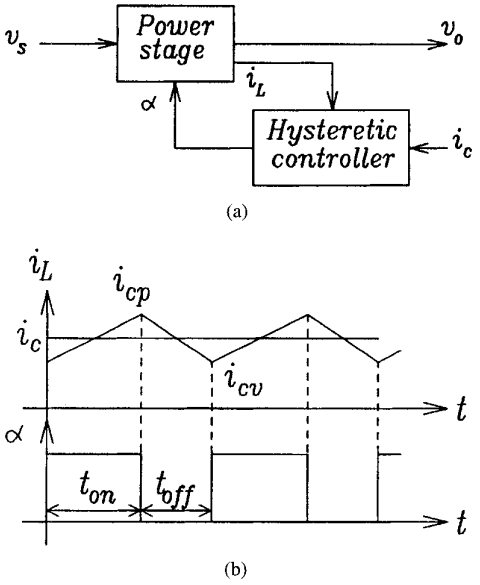

Fig. 1. Hysteretic current-programmed control. (a) Block diagram. (b) Typical waveforms.

The switching power supply system under hysteretic current-programmed control, however, is a nonlinear dynamic system. Such a system may be stable in the vicinity of the operating point but may not be stable when the system undergoes a large perturbation. Therefore, the small-signal model cannot provide the stability information when the system is subject to a large-signal disturbance or a large parameter variation. An example of this circumstance is illustrated in [9]. Therefore, a large-signal model is essential to study the global dynamic characteristics of the switching converter under hysteretic current-programmed control and to design robust and high-performance switching power supply. Unfortunately, the large-signal characteristics of the hysteretic current-programmed control has never been investigated.

The objective of this paper is 1) to establish the large-signal model of the hysteretic current-programmed buck, boost, and buck-boost converters so that the large-signal characteristics can be analyzed, and 2) to derive the small-signal transfer function based on the proposed large-signal model. The paper is organized as follows: In the next section, a technique to establish the large-signal dynamic model for the hysteretic current-programmed boost converter is proposed, and the large-signal characteristics are analyzed. In Section III, the small-signal transfer function is derived from the large-signal

model. The result shows that there is a right-half plane (RHP) zero in the control-to-output transfer function for the boost converter. The RHP zero is the same as that in the direct duty ratio control. The same technique is also used to derive the large-signal model for the hysteretic current-programmed buck and buck-boost converters in Section IV. The small-signal transfer functions are also derived in that section. In Section V, an experimental hysteretic current-programmed boost converter is breadboarded to verify the large-signal and small-signal models proposed in the paper. Section VI is the conclusion.

II. Large-Signal Model for Boost Converter under Hysteretic Current-Programmed Control

In this section, the large-signal low-frequency model for the hysteretic current-programmed boost converter is proposed, and the large-signal characteristics are analyzed.

Two assumptions are made in the following analysis.

1) *Small-Ripple Assumption:* The supply voltage, $v_s(t)$, the capacitor voltage $v_c(t)$, and the inductor current $i_L(t)$ at time t are well-approximated by their average values, v_s, v_o, and i_L, respectively.
2) *Slow-Variation Assumption:* The average value of the v_s, v_c, and i_L does not vary significantly over any averaging interval of length T. In other words, they vary substantially more slowly than one-half of the switching frequency.

These two assumptions are generally satisfied in well-designed high-frequency switching converters operating in continuous conduction mode.

For the boost converter shown in Fig. 2(a), the switch Q is on for time period t_{on} and off for period t_{off}. The equivalent circuits for these two intervals are given in Fig. 2(b) and (c). The state-space differential equations for on-state and off-state are the following: For on state ($0 \le t \le t_{on}$)

$$\begin{cases} L\dfrac{di_L(t)}{dt} &= v_s(t) \\ C\dfrac{dv_o(t)}{dt} &= -\dfrac{v_o(t)}{R} \end{cases} \tag{1}$$

and for off state ($t_{on} \le t \le t_{on}+t_{off}$)

$$\begin{cases} L\dfrac{di_L(t)}{dt} &= v_s(t)-v_o(t) \\ C\dfrac{dv_o(t)}{dt} &= -i_L(t)-\dfrac{v_o(t)}{R} \end{cases} \tag{2}$$

where $v_s(t)$, $v_o(t)$, $i_L(t)$ are instantaneous value of the supply voltage, output voltage, and inductor current.

According to the basic idea of the state-space averaging method [3], the averaged state-space differential equation can be obtained by multiplying (1) by $t_{on}/(t_{on}+t_{off})$, multiplying (2) by $t_{off}/(t_{on}+t_{off})$, and adding the above two expressions together. The result can be expressed as

$$\begin{cases} L\dfrac{di_L}{dt} &= v_s-\dfrac{t_{off}}{t_{on}+t_{off}}v_o \\ C\dfrac{dv_o}{dt} &= \dfrac{t_{off}}{t_{on}+t_{off}}i_L-\dfrac{v_o}{R} \end{cases} \tag{3}$$

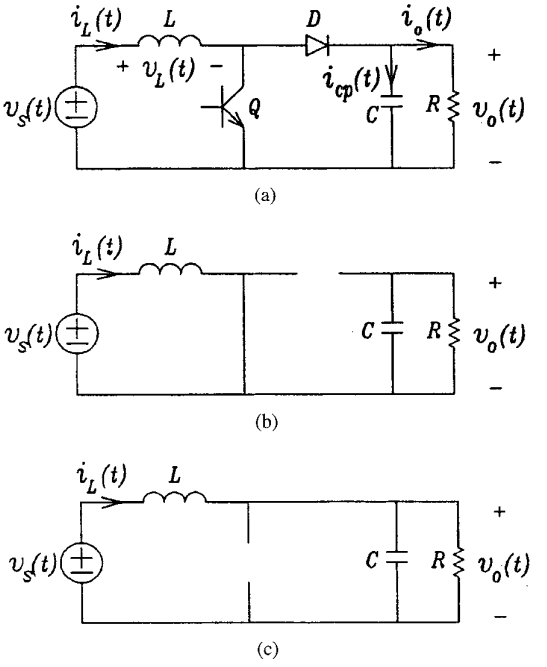

Fig. 2. (a) Boost converter topology and its (b) on-state and (c) off-state equivalent circuit.

where v_s, v_o, and i_L are averaged value. Define the duty ratio α as

$$\alpha = \frac{t_{on}}{t_{on}+t_{off}}. \tag{4}$$

Equation (3) can be rewritten as

$$L\frac{di_L}{dt} = v_s-(1-\alpha)v_o \tag{5a}$$

$$C\frac{dv_o}{dt} = (1-\alpha)i_L-\frac{v_o}{R}. \tag{5b}$$

The above state-space equations are valid for both constant switching frequency and variable switching frequency because no constraint is applied to $t_{on}+t_{off}$ in the above derivation.

In the hysteretic current-programmed control, when the inductor current reaches $i_c+\Delta I/2$, the switch is turned off, and the inductor current falls. When the inductor current falls to $i_c-\Delta I/2$, the switch is turned on again. Therefore, the average value of the inductor current i_L is controlled tightly by the command signal i_c. It can be assumed that the average inductor current equals to the command signal, i.e.,

$$i_L = i_c. \tag{6}$$

In the hysteretic current-programmed control, the duty ratio is no longer the control input and can be expressed by other circuit variables from (5b) as

$$\alpha = 1-\frac{\dfrac{v_o}{R}+C\dfrac{dv_o}{dt}}{i_L}. \tag{7}$$

Substituting (6) and (7) into (5a) and making some rearrangement, the following equation is derived

$$Cv_o\frac{dv_o}{dt}+\frac{v_o^2}{R} = v_si_c-Li_c\frac{di_c}{dt}. \tag{8}$$

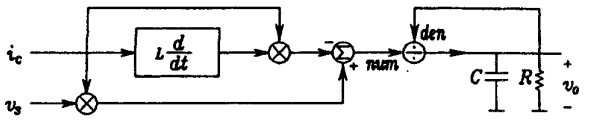

Fig. 3. Block diagram of the large-signal model of the hysteretic current-programmed boost converter.

The above equation describes the large-signal low-frequency characteristics of the boost converter under hysteretic current-programmed control. Its block diagram expression is given in Fig. 3, where the symbol $\times$ inside a circle denotes a multiplier, the symbol Σ inside a circle denotes an adder, and the symbol $\div$ inside a cycle denotes a divider with the terminal *num* as the numerator and terminal *den* as denominator. The block $L(d/dt)$ denotes the differential operation with gain L.

One way to obtain the large-signal characteristics of the hysteretic current-programmed boost converter is to integrate (8) directly, using Runge–Kuta algorithm [4]. Another way is to enter the large-signal model of Fig. 3 into a control system analysis software, such as Tutsim [5], to obtain the large-signal response of the system.

The model, expressed by (8) or Fig. 3, shows that the boost converter under the hysteretic current-programmed control becomes a first-order system. This is understandable because the averaged inductor current follows the control signal so tightly that it is no longer a state variable. This fact is also beneficial because it is always easier to keep a first-order system stable.

Another phenomenon that can be observed from (8) is that the output voltage will be affected not only by the control signal i_c, but also by its change rate, di_c/dt. The effect of the change rate is such that it will always oppose the effect of the control signal i_c. For example, when the control signal has a step increase from i_{c1} to i_{c2}, the steady-state output voltage will increase from V_{o1} to V_{o2}. But during the rising period of i_c, the right side of (8) becomes negative, and the output voltage will at first drop a little bit and then rise toward the new steady-state value. Fig. 4 gives the response of the output voltage when the control signal, i_c, steps from 2 to 5 A. The first-order response is shown obviously. The dip of the output voltage is also observed clearly, as shown in Fig. 4(b). Other circuit parameters used in the simulation are $V_s = 10$ V, $L = 290$ μH, $C = 760$ μF and R = 10 Ω.

This prediction can be explained qualitatively from the operation of the hysteretic current-programmed boost converter. When the control signal increases suddenly, the average inductor current has also to increase immediately. Therefore, the active switch has to conduct for a longer time so that the inductor current can build up, and the filter capacitor has also to discharge for longer time. The consequence is that the output voltage will at first dip a little bit until the inductor current is increased and recharges the output capacitor at a higher current level. In the small-signal domain, this dip implies that there is a right-half-plane zero in the control-to-output transfer function, as will be shown in the next section.

When the supply voltage has a step change from $v_{s1} = 10$ V to $v_{s2} = 15$ V, the response of the output voltage is plotted

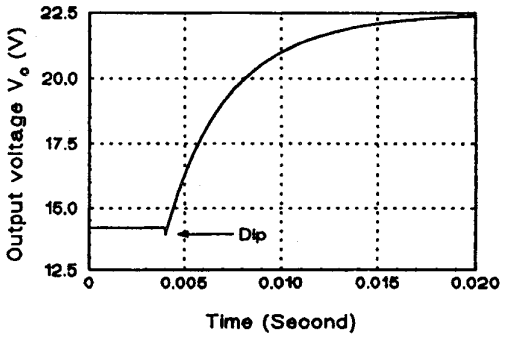

(a)

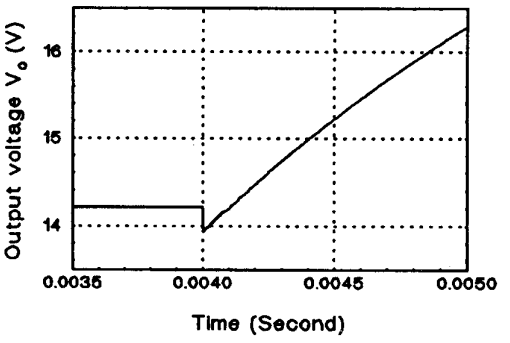

(b)

Fig. 4. Response of the output voltage v_o with step change of control signal i_c. (a) General version. (b) Enlarged version.

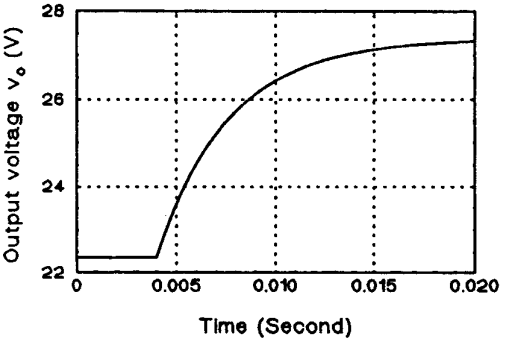

Fig. 5. Response of the output voltage v_o with step change of supply voltage v_s.

in Fig. 5 for $C = 760$ μF, $R = 10$ Ω, and $I_c = 5$ A. First-order response is clearly observed. Since the inductor current is controlled tightly, the output voltage will increase when v_s increases.

In this section, the large-signal model of the boost converter under hysteretic current-programmed control is proposed. It shows that the boost converter under hysteretic current-programmed control becomes a first-order system. The output voltage is affected by both the control signal and its change rate. The small-signal transfer function can be obtained from the large-signal model under small-signal assumption, which is the subject of the next section. The same technique can also be used to derive the large-signal model of the hysteretic current-programmed buck and buck-boost converters, as will be discussed in Section IV.

III. Small-Signal Model for Boost Converter under Hysteretic Current-Programmed Control

The small-signal transfer function of the hysteretic current-programmed boost converter can be derived from the large-signal model, (8), proposed in the previous section. Here it is assumed that the uppercase letter denotes the steady-state value, the lowercase letter denotes the averaged value, and the lowercase letter with a hat, $\hat{}$, above it denotes the small-signal disturbance, i.e., $x = X + \hat{x}$, with $\hat{x} \ll X$. Substituting

$$\begin{aligned} v_o &= V_o + \hat{v}_o \\ i_c &= I_c + \hat{i}_c \\ v_s &= V_s + \hat{v}_s \end{aligned} \tag{9}$$

into (8) and neglecting terms containing the product of the small-signal disturbance, also noticing that the derivative of the steady-state value is zero, the following equation is obtained

$$CV_o \frac{d\hat{v}_o}{dt} + \frac{2V_o}{R}\hat{v}_o = I_c\hat{v}_s + V_s\hat{i}_c - LI_c\frac{d\hat{i}_c}{dt}. \tag{10}$$

The steady-state relation of the hysteretic current-programmed boost converter is

$$V_sI_c = \frac{V_o^2}{R}. \tag{11}$$

Taking the Laplace transformation of (10) and also noticing the relation of (11), the small-signal transfer function of the hysteretic current-programmed boost converter can be derived as

$$V_o(s) = \frac{\frac{1}{2D'}V_s(s) + \frac{R}{2}D'\left(1 - \frac{sL}{D'^2R}\right)I_c(s)}{1 + \frac{1}{2}sRC} \tag{12}$$

where D' is defined as $D' = V_s/V_o$.

It is shown clearly that there is a right-half-plane zero in the control-to-output transfer function. The location of the zero is the same as that of the duty ratio control [3] and the peak current control [6], [7]. The reason for this phenomenon is the contradiction between the increasing of the inductor current and the increasing of the output voltage simultaneously in the boost converter. No matter what kind of control law is employed, the active switch has to conduct a longer time to increase the average inductor current, and the filter capacitor has to discharge for a longer time and the output voltage will dip during this period. Therefore, the right-half-plane zero of the boost converter is always present for various kinds of control law, and it cannot be shifted to the left-half side of the s-plane.

The block diagram of the small-signal model is given in Fig. 6. This model can be used to design the feedback compensator to obtain a wideband and stable closed-loop system.

It is noted that in the above derivation, the sample-and-hold effect that introduces a time delay $e^{-t_{on}s}$ is not considered. Therefore, the above model is accurate in the low-frequency range, i.e., the changing of the control signal, supply voltage, is much slower as compared with the switching period. Extra phase delay will be introduced at high frequency.

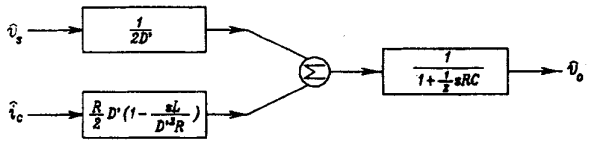

Fig. 6. Block diagram of the small-signal model of the hysteretic current-programmed boost converter.

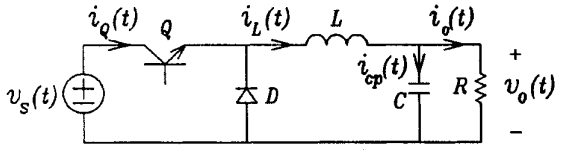

Fig. 7. Buck converter topology.

In the previous section and this section, the large-signal and small-signal models of the hysteretic current-programmed boost converter are proposed. Its dynamic characteristics can be analyzed according to the models. The same technique can also be used to derive the large-signal model of the hysteretic current-programmed buck and buck-boost converters.

IV. Dynamic Models for Buck and Buck-Boost Converters

In this section, the large-signal models of the hysteretic current-programmed buck and buck-boost converters are established using the same technique as above. The small-signal transfer functions are also derived from the large-signal models.

A. Buck Converter

The topology of the buck converter is given in Fig. 7. The averaged state space equation can be derived as

$$L\frac{di_L}{dt} = \alpha v_s - v_o \tag{13a}$$

$$C\frac{dv_o}{dt} = i_L - \frac{v_o}{R} \tag{13b}$$

where α is the duty ratio defined by (4).

In the hysteretic current-programmed buck converter, the average inductor current follows the control signal tightly, (6). Substituting (6) into (13b), the large-signal model for the buck converter under the hysteretic current-programmed control can be expressed as

$$C\frac{dv_o}{dt} + \frac{v_o}{R} = i_c. \tag{14}$$

Equation (14) shows that under the hysteretic current-programmed control, the buck converter becomes a first-order linear system, and the output voltage is independent of the supply voltage. These are very good features. This observation can be explained as follows. In the buck converter, the inductor is connected directly to the output. The hysteretic current-programmed control changes the inductor into a current source that drives directly the output capacitor and the load resistor, as shown in Fig. 8. As long as the averaged inductor current

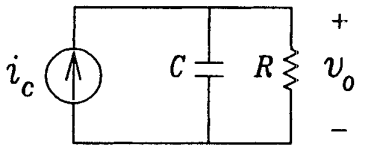

Fig. 8. Large-signal model of hysteretic current programmed buck converter.

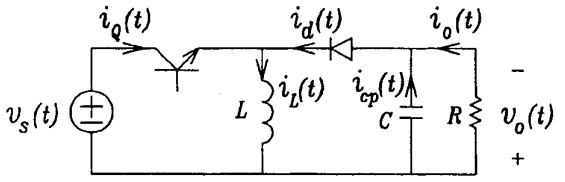

Fig. 9. Buck-boost converter topology.

i_L, i.e., the control current i_c, does not change, the averaged output voltage will be independent of the supply voltage.

The small-signal transfer function can be derived directly from (14) as

$$v_o(s) = \frac{Ri_c(s)}{1 + sRC}. \tag{15}$$

B. Buck-Boost Converter

The topology of the buck-boost converter is given in Fig. 9. The averaged state-space differential equation can be derived as

$$L\frac{di_L}{dt} = \alpha(v_s + v_o) - v_o \tag{16a}$$

$$C\frac{dv_o}{dt} = (1-\alpha)\, i_L - \frac{v_o}{R} \tag{16b}$$

where α denotes the duty ratio. In the hysteretic current-programmed buck-boost converter, the averaged inductor current equals the control signal, as described by (6), and the duty ratio α is not an independent variable but can be expressed from (16b) by other circuit variables as

$$\alpha = 1 - \frac{\frac{v_o}{R} + C\frac{dv_o}{dt}}{i_L}. \tag{17}$$

Substituting (17), (6) into (16a), the large-signal dynamic equation for the buck-boost converter under hysteretic current-programmed control can be derived as

$$C(v_s + v_o)\frac{dv_o}{dt} + \frac{v_o(v_o + v_s)}{R} = v_s i_c - Li_c\frac{di_c}{dt}. \tag{18}$$

The dynamic response of the output voltage under large-signal variation of the operating point can be obtained by integrating (18). Similar to the boost converter under hysteretic current-programmed control, the dynamic output voltage of buck-boost converter is also affected by both the control signal, i_c, and by its change rate, di_c/dt. The effect of di_c/dt will always try to oppose the effect of i_c. This phenomenon implies a right-half-plane zero in the control-to-output transfer function.

The small-signal transfer function of the buck-boost converter under the hysteretic current-programmed control can be derived by small-signal perturbation, i.e., (9). Substituting (9) into (18) and neglecting the terms containing the product of small-signal disturbance, the small-signal dynamic equation is obtained as

$$C(V_s + V_o)\frac{d\hat{v}_o}{dt} + \frac{2V_o + V_s}{R}\hat{v}_o = \left(I_c - \frac{V_o}{R}\right)\hat{v}_s + V_s\hat{i}_c - LI_o\frac{d\hat{i}_c}{dt}. \tag{19}$$

The steady state relation is

$$\frac{V_o(V_o + V_s)}{R} = V_s I_c. \tag{20}$$

Take the Laplace transformation of (19) and notice the steady-state relation of (20), the small-signal transfer function of the hysteretic current-programmed buck-boost converter is obtained

$$V_o(s) = \frac{1}{1+D}\,\frac{\frac{D^2}{D'}V_s(s) + D'R\left(1 - \frac{sDL}{D'^2R}\right)I_c(s)}{1 + \frac{sRC}{1+D}} \tag{21}$$

where D is the steady-state duty ratio and $D' = 1 - D$.

It is noted from (21) that there is a right-half-plane zero in the control-to-output transfer function. The frequency of this zero is the same as that of the duty ratio control [3] and the peak current control [6]. This zero is induced by the physical contradiction of increasing the average inductor current and average output voltage simultaneously in the buck-boost converter.

The large-signal and small-signal models of the hysteretic current-programmed buck, boost, and buck-boost converters are proposed. Because the averaged inductor current is controlled tightly, the state variable associated with the inductor current no longer exists and the system becomes first order. The right-half-plane zero is present for the boost and buck-boost converters under hysteretic current-programmed control because of the physical contradiction of simultaneously increasing the average inductor current and output voltage. In the large-signal time domain, this contradiction is represented by the fact that the effect of the change rate of the control signal always tries to oppose the effect of the control signal itself.

V. Experimental Verification

A boost converter under hysteretic current-programmed control is breadboarded to verify the validity of the large-signal and small-signal models proposed in the paper. The experimental circuit is given in Fig. 10. The objective of the experimental prototype is to compare the measured large-signal and small-signal response with the theoretical prediction. The circuit parameters are the same as those used in the large-signal analysis, i.e., $L = 290\,\mu$H, $C = 760\,\mu$F, $R = 10$ W, and $V_s = 10$ V.

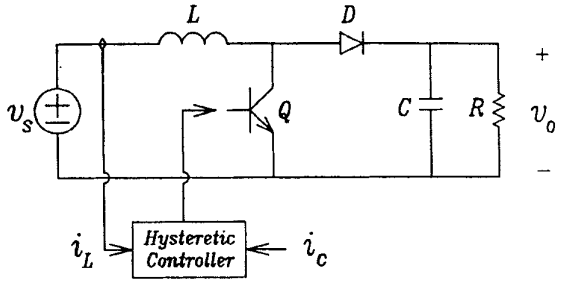

Fig. 10. Block diagram of the experimental circuit.

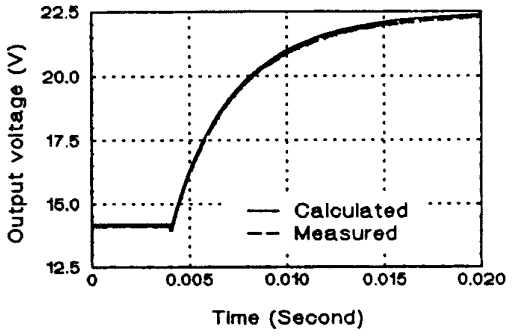

(a)

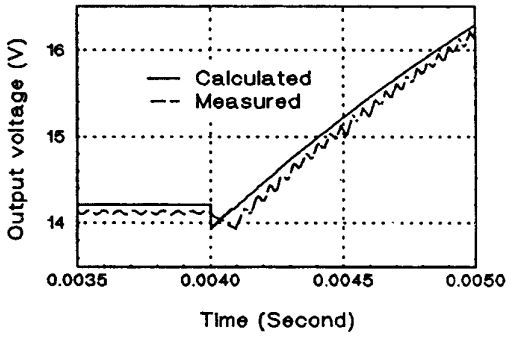

(b)

Fig. 11. Large-signal output voltage response when control signal i_c steps. (a) Output voltage. (b) Enlarged version.

A. Large-Signal Response

In the large-signal response measurement, the Nicolet 310 digital scope is used to record the response of the output voltage, the inductor current, and the control signal. The recorded data is then transferred to a computer and plotted at the same graph against the simulated curve.

Fig. 11(a) gives the measured and the calculated responses of the output voltage when the control signal steps from 2 to 5 A. The measured voltage is smoothed at every 5 points. It is shown that the measured data and the calculated data are very close. The dip of the output voltage immediately after the step change of control signal i_c is shown clearly in the enlarged version in Fig. 11(b). Fig. 12 gives the measured control signal i_c and the measured inductor current, i_L. Obviously, the inductor current follows the control signal tightly and accurately. These two curves cannot be distinguished from each other if plotted in the same graph. This shows that the assumption $i_L = i_c$ is valid for the hysteretic current-programmed control.

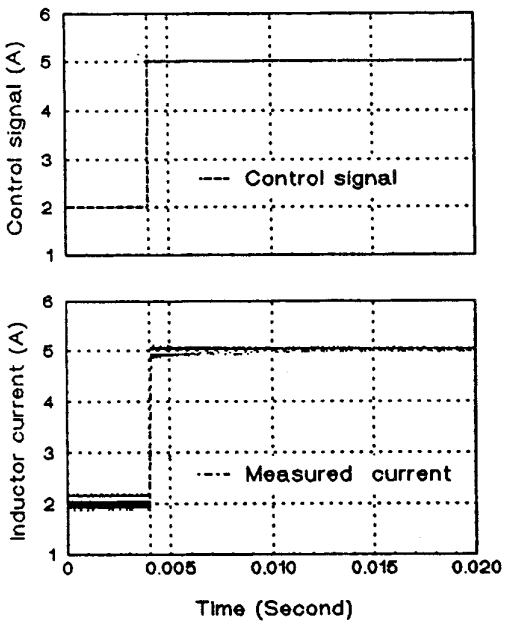

Fig. 12. Large-signal inductor current response when control signal i_c steps.

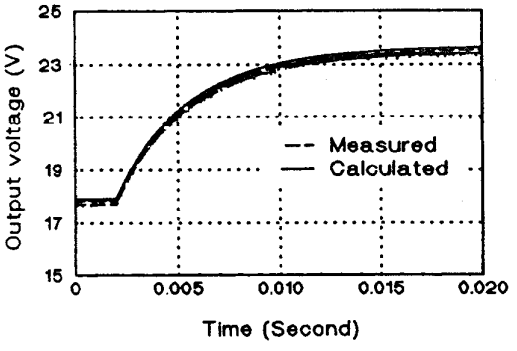

Fig. 13. Large-signal output voltage response when supply voltage v_s steps.

The effect of the large-signal disturbance of the supply voltage is also studied. Fig. 13 shows the output voltage response when the supply voltage steps from 10 to 15 V at $I_c = 4$ A. The calculated curve is also plotted at the same graph. The measured response is very close to the calculated one.

The above measurement shows that the large-signal model proposed in the paper can predict accurately the dynamic response of the output voltage under large-signal variation of the operating point.

B. Small-Signal Response

The small-signal control-to-output transfer functions, $V_o(s)/I_c(s)$, and audiosusceptibility, $V_o(s)/V_s(s)$, of the boost converter under hysteretic current-programmed control, are also measured and compared with the theoretical prediction (12). The circuit parameters are the same as before, and the operating condition is $V_s = 10$ V and $V_o = 20$ V ($I_c = 4$ A).

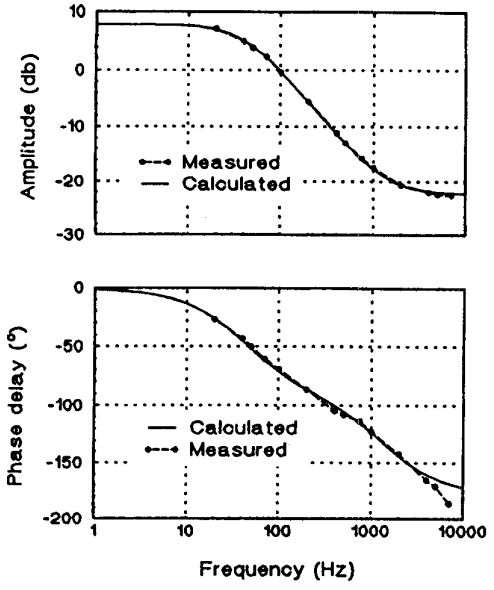

Fig. 14. Measured and calculated small-signal control-to-output transfer functions.

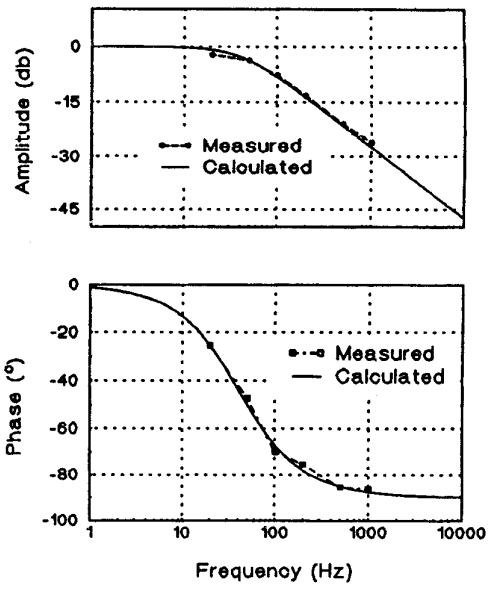

Fig. 15. Measured and calculated audiosusceptibility.

Fig. 14 gives the measured and calculated control-to-output transfer functions. The phase delay of the control-to-output transfer function is well beyond $-90°$ and actually goes to $-180°$, which indicates the presence of the right-half-plane zero. As the signal frequency approaches the switching frequency, the measured delay is larger than the predicted because of the sampling effect. The input-to-output transfer function (audiosusceptibility) is also measured and plotted in Fig. 15. The phase delay approaches $-90°$ when the signal frequency increases. This phenomenon indicates that the boost converter under hysteretic current-programmed control is a first-order system. It is clear that the measured small-signal transfer functions are very close to the calculated one.

The experimental results provided in this section show that the large-signal and small-signal models, (8) and (12), proposed in the paper can predict the dynamic characteristics of the hysteretic current-programmed boost converter accurately. The measured data is very close to the theoretical prediction.

VI. Conclusion

In this paper, a method is proposed to derive the large-signal models of the hysteretic current-programmed buck, boost, and buck-boost converters under the assumption that the inductor current is controlled tightly in the hysteretic current-programmed control. The procedure to obtain the large-signal model is outlined, and the model is expressed as a single differential equation. The large signal characteristics are analyzed for the first time. The analysis shows that the output voltage for the hysteretic current-programmed buck converter is independent of the supply voltage, and the output voltage of hysteretic current-programmed boost and buck-boost converters is affected by both the control signal and its change rate.

The small-signal transfer functions of the hysteretic current-programmed buck, boost, and buck-boost converters have also been derived from the large-signal models. It is demonstrated that there is a right-half-plane zero in the control-to-output transfer function of hysteretic current-programmed boost and buck-boost converters. This right-half-plane zero is inherently present because of the contradiction of simultaneously increasing the inductor current and the output voltage. The position of the right-half-plane zero is the same as that of direct duty ratio control and peak current-programmed control. This is a correction to the previous results about small-signal transfer function of the boost and buck-boost converters under hysteretic current-programmed control.

A boost converter under the hysteretic current-programmed control is breadboarded to verify the large-signal model and the small-signal transfer function proposed in the paper. The measurements and the theoretical predictions are very close. The experimental result also shows that the averaged inductor current follows the control signal tightly.

The large-signal model presented in this paper gives a global view of the dynamic response of the hysteretic current-programmed converters, which enables the designer to understand the limits of the system and helps the designer to achieve robust control. The small-signal model is also a useful guide to design the compensation network. A hysteretic current-programmed switching power supply with global stability can be obtained by the help of the proposed models.

References

[1] A. Capel, G. Ferrante, D. O'Sullivan, and A. Weinberg, "Application of the injected current model for the dynamic analysis of switching regulators with the new concept of LC^3 modulator," in *IEEE Power Electron. Spec. Conf. Rec.*, 1978, pp. 135–147.

[2] R. Redl and N.O. Sokal, "Current-mode control, five different types, used with the three basic classes of power converters: Small-signal ac and large-signal dc characterization, stability requirements, and implementation of practical circuits," in *IEEE Power Electron. Spec. Conf. Rec.*, 1985, pp. 771–785.

[3] R. D. Middlebrook and S. Ćuk, "A general unified approach to modeling switching-converter power stages," in *IEEE Power Electron. Spec. Conf. Rec.,* 1976, pp. 18–34.
[4] W. H. Press, B. P Flannery, S. A. Teukolsky, and W. T. Vetterling, *Numerical Recipes: The Art of Scientific Computing.* New York: Cambridge Univ. Press, 1992.
[5] W. E. Reynolds and J. Wolf, *TUTSIM User's Manual,* 1987.
[6] S. P. Hsu, A. Brown, L. Rensink, and R. D. Middlebrook, "Modeling and analysis of switching dc-to-dc converters in constant-frequency current-programmed mode," in *IEEE Power Electron. Spec. Conf. Rec.,* 1979, pp. 284–301.
[7] R. D. Middlebrook, "Modeling current-programmed buck and boost regulators," *IEEE Trans. Power Electron.,* vol. 4, no. 1, pp. 36–52, Jan. 1989.
[8] R. Redl, "Small-signal high-frequency analysis of the free-running current-mode-controlled converter," in *IEEE Power Electron. Spec. Conf. Rec.,* 1991, pp. 897–906.
[9] R. Erickson, S. Cuk, and R. D. Middlebrook, "Large-signal modeling and analysis of switching regulators," in *Power Electron. Spec. Conf. Rec.,* 1982, pp. 240–250.

Yan-Fei Liu (M'94) received the B.Sc. and M.Sc. degrees in electrical engineering from Zhejiang University, Hangzhou, People's Republic of China, in 1984 and 1987, respectively, and the Ph.D. degree from Queen's University, Kingston, Ontario, Canada, in 1994.

He was Assistant Professor at Zhejiang University from 1987 to 1990. From September 1990 to February 1994, he was a Research and Teaching Assistant at Queen's University and Adjunct Instructor from September 1993 to December 1993. He is currently with the Power Group at Bell Northern Research, Ltd., Ottawa, Ontario, Canada. His research interests include new circuit configurations of soft switching converters for dc-to-dc converters and power-factor correction circuits, control techniques to improve the dynamic performance of PWM switching converters, dynamic modeling of switching power converters, computer simulation of analogue circuits, power electronic circuits, and power-factor correction circuits.

Paresh C. Sen (M'67–SM'74–F'89) was born in Chittagong, Bangladesh. He received the B.Sc. degree (Hons.) in physics and the M.Sc. degree (Tech.) in applied physics from the University of Calcutta, India, in 1958 and 1961, respectively. He received the M.A.Sc. and the Ph.D. degrees in electrical engineering from the University of Toronto, Ontario, Canada, in 1965 and 1967, respectively.

He is Professor of Electrical Engineering at Queen's University, Kingston, Ontario, Canada. He has written more than 90 research papers in the general area of power electronics and drives. He has served as Associate Editor of IEEE TRANSACTIONS ON INDUSTRIAL ELECTRONICS AND CONTROL INSTRUMENTATION (IEICI Society) on Power Electronics (1979–1980) and Energy Systems (1980–1982) and is the author of two books, *Thyristor DC Drives* (New York: Wiley, 1981) and *Principles of Electric Machines and Power Electronics* (New York: Wiley, 1988). His fields of interest include power electronics and drives, microcomputer control of electric drives systems, modern control techniques for high-performance drive systems, and switching power supplies.

Dr. Sen has served on program committees of many IEEE and international conferences and has organized and chaired many technical sessions. At present, he is an active member of the Industrial Drives Committee and the Static Power Converter Committee of the IEEE Industry Applications Society. He is also a member of the International Steering Committee on International Conference on Electric Drives (ICED). He is internationally recognized as a specialist in power electronics and drives and has received a Prize Paper Award from the Industrial Drive Committee for technical excellence at the Industry Applications Society Annual Meeting in 1986.